Separation and Purification Technology 337 (2024) 126343

Contents lists available at ScienceDirect

Separation and Purification Technology

journal homepage: www.elsevier.com/locate/seppur

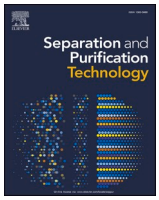

Effect of feed concentration in solvent/anti-solvent precipitation fractionation of lignin: Impact on lignins structure-property correlations

Arulselvan Ponnudurai *, Peter Schulze, Andreas Seidel-Morgenstern, Heike Lorenz

Max-Planck-Institute for Dynamics of Complex Technical Systems, Magdeburg, Germany

ARTICLE INFO

Editor: B. Van der Bruggen

Keywords:
Lignin precipitation fractionation
Structure-property relationship
Polydispersity
Phase separation
Glass transition temperature

ABSTRACT

Technical lignins are relatively heterogeneous and structurally not fully understood, which hinders their commercialization. This study involves the precipitation fractionation of organosolv (OS) lignin into different molecular weight (MW) classes by stepwise addition of water as an anti-solvent in acetone/water mixtures with varying feed lignin concentrations of 5, 10, and 15 wt. % in the lignin/solvent/anti-solvent mixture. Characterization of the obtained lignin fractions by SEC-MALS, TM-DSC, and ^{31}P NMR revealed MW classes in a broad range from 2050 to 26500 g mol^{-1}, glass transition temperatures between 68 and 201 °C and the presence of different amounts of hydroxyl groups. The results verify that besides the acetone/water gradient, the lignin concentration has a major influence on the fractionation outcome. We demonstrate the significant impact of different OS lignin concentrations on the solubility of such polydisperse system and hereby establish an additional way to tune the molecular weight of lignin fractions and their related physico-chemical properties.

1. Introduction

Lignocellulosic biomass (LCB), derived from plants, is the most abundant and sustainable solid carbon source available on the planet [1,2]. It consists of two carbohydrate polymers, cellulose and hemicellulose, and a non-carbohydrate aromatic heteropolymer called lignin, which has a rich and complex structure and is present in the vascular tissue walls of plants. The composition of lignin varies among plant species and even within different tissues of the same plant [1–3]. The coupling of radicals between the three major lignin monomers leads to the formation of a diverse range of inter-unit linkages, primarily involving carbon–oxygen bonds (as β-O-4, α-O-4 and 4-O-5 bonds) and carbon–carbon bonds (as β-β, β-5, β-1, and 5–5 bonds). The β-O-4 bonds are the most common ether linkages in lignin. They account for 40–65 % of all inter-unit linkages [4–6]. Furthermore, lignin monomers comprise several functional groups, including aliphatic, phenolic hydroxyl, carboxylic, carbonyl, and methoxy groups. Thus, the structure of lignin is further complexed by hydrogen bonds between neighboring oxygen containing groups and also π-π interactions between aromatics, which alter and influence lignins polarity, solubility and reactivity [7–9]. The presence and proportion of these functional groups and chemical linkages depend on the agricultural source and extraction methods employed [5,6].

Lignin accounts for up to 25 % of the total land-based biomass and consequently displays a promising candidate as the primary renewable source for aromatic chemicals in the future, which has led to an increased interest in lignin biorefinery concepts [10,11]. Currently produced technical lignins like Kraft lignin or lignosulfonates are obtained by relatively harsh pulping conditions and contain amounts of impurities as e.g. polysaccharides from lignin-carbohydrate complexes, metal salts, and sulfur [12–14]. However, alternative techniques for producing greener pulp and more pure and reactive lignins have been established since the early 20th century and have been continuously improved, e.g. the OS pulping process. Hereby, an aqueous organic solvent, frequently in combination with a small amount of an inorganic acid or base as a catalyst is used to extract pure lignin from the fibers, as recently studied by various groups [11,15–19]. Especially, the isolation of lignins from the acetone OS (Fabiola™) process has been shown to result in high purities and an overall energy-efficient process [11]. Despite its potential, the use of technical (OS) lignin in material applications is still limited. The heterogeneous structure and wide molecular weight distribution (MWD) of lignin can have a significant impact on its potential applications in materials [1,20,21]. Numerous studies have demonstrated the utilization of lignin for further usage, but the aforementioned broad distribution of its MW, lignins intrinsic functional diversity, and linkages often limits comprehensive, efficient and higher

* Corresponding author.
E-mail address: ponnudurai@mpi-magdeburg.mpg.de (A. Ponnudurai).

https://doi.org/10.1016/j.seppur.2024.126343
Received 3 November 2023; Received in revised form 21 December 2023; Accepted 6 January 2024
Available online 9 January 2024

value utilization [1,21].

A promising research area involves the development of well-defined, purified lignin fractions with narrow distribution (MW and functional distribution), which could potentially enhance the value and consequently lead to new market options. Thus, it is crucial to establish selective, and cost-efficient (fractionation) methods for the retrieval and valorization of lignin [14,22–27]. Lignin with a low MW typically possesses more reactive functional groups, resulting in a higher antioxidant performance [10,25]. In addition, low MW lignin fractions with higher amounts of functionalities have been investigated with respect to bio-based polymer blends [28–30]. Contrarily, lignin with a higher MW performs well as a precursor material for carbon fibers [29,31]. Kanhere et al. reported that high MW lignin fractions (with low dispersity) and high glass transition temperature (T_G) displayed excellent stability during dry spinning and revealed high carbon fiber strength. Hereby, the processing temperature needs to be below the T_G of lignin as in other case the fibers may start to undesirably fuse. In this regard, control not over only MW and MWD, but also over the T_G would be beneficial [31–34].

Various fractionation methods have been reported to date, including membrane-assisted filtration, acidification, and sequential solvent fractionation [10,22,24,35–39]. Ultrafiltration can provide a narrow distribution of lignin classes as reported. However, membrane fouling and expensive instrumentation made this approach unsuitable for prospective industrial implementation [40]. Acidification, by varying the pH from high to low, revealed a simpler way to classify alkali-soluble lignin by size. This approach is comparably simpler, but the usage of strong and harmful acids is economically not attractive and limits the scalability of such a fractionation process [37].

The basic principle of (solvent) fractionation techniques is the subdivision of the polymer sample into fractions due to the different solubility of the molecular species of different MWs, respectively by changing the dissolution power [41]. By varying the solvent/anti-solvent system or temperature the dissolution power can be manipulated. A precipitation fractionation is conducted once the dissolution power is decreased by enrichment of an anti-solvent in a solvent/anti-solvent mixture or by varying the temperature (mostly a lowering). Hereby, the MW decreases from the first fractions towards the last. An extraction fractionation is conducted once the dissolution power increases, respectively by sequential or continuous enrichment of the solvent in the fractionation mixture or by a rise of the temperature. During the extraction fractionation, the MW increases stepwise from the first fraction [41].

It is well known, that the Hildebrand (and Hansen) solubility parameter (δ) can give a good indication of the solubility for substances and solvents. Hereby, similar values of δ represent good solubility and miscibility between solvent and solute [10,42,43]. Mohan et al. and others found depending on the isolated lignin structure a range of solubility parameter values between 22.5 and 27 $MPa^{1/2}$ [9,44]. The group of Sixta reported for OS hardwood beech wood lignin as used in this work a value of 25.5 $MPa^{1/2}$ [45].

Sequential solvent fractionations using multiple organic solvents (e.g. ethyl acetate, ethanol, acetone, or methanol) have shown to produce classes of lignins with narrower dispersity [2,16,24,38,46,47]. This is eligible on a lab scale but complicates and limits the scaling up due to various solvent usages with its consequent solvent recycling. This limitation can be overcome by fractionating lignin in one aqueous solvent system (e.g. with acetone) and stepwise adding water as an anti-solvent as mentioned above [20,22,23,26,48]. Acetone/water is a practicable solvent system for this investigation, not only for the lignin fractionation but also for the extraction of lignin from LCB, and is considered as green, non-toxic, and easily recyclable [11].

In this paper, we have deeper investigated the potential of the lignin precipitation fractionation in acetone/water as solvent/anti-solvent system to enhance the fundamental understanding towards a realistic and industrially applicable fractionation process design. An increase in the feed lignin concentration in the fractionation process can potentially raise its overall yield and productivity significantly. Hence, the solvent/anti-solvent fractionation was investigated starting with three different initial feed lignin concentrations. Hereby, the fractionation steps, respectively the acetone concentration in the lignin/solvent/anti-solvent mixture in each step, were kept equal to compare the fractions in terms of their chemical and physical properties. These comprise MWD and MW analysis, elemental analysis, T_G analysis, functional group determination, and antioxidant activity. Currently, to the best of the author's knowledge, no characterization and comparison of lignin fractions obtained through anti-solvent precipitation fractionation from different lignin feed concentrations under otherwise identical conditions have been reported for OS lignin in the literature. Furthermore, the importance and therefore the necessity of understanding the phase behavior of lignin and the phase separation process of such a polydisperse system will be emphasized and discussed.

2. Materials and methods

2.1. Materials

The OS beech wood lignin has been produced by the lignocellulose biorefinery pilot plant at Fraunhofer CBP in Leuna, Germany. It processes up to 70 kg of wood chips per batch, whereby lignin precipitation from the pulping liquor is performed continuously by the LigniSep process. Detailed process conditions and parameters can be found in previous works [11,15].

All reagents used in this work were commercially purchased and used as received. Tap water was purified using a Millipore filter system (resistivity 18.2 MΩ cm, total organic carbon (TOC) 3 ppb).

2.2. Stepwise anti-solvent precipitation fractionation

The used fractionation method is based on a previously published study [20]. Besides a 10 wt. % (5 g lignin / 45 g solvent), the impact of a 5 and 15 wt. % (2.5 or 7.5 g lignin and 47.5 or 42.5 g solvent) feed lignin solution on the fractionation was investigated. Eight consecutive anti-solvent fractionation steps have been proceeded to obtain eight main fractions (F_1 to F_8) from the starting lignin material (parent lignin) leading to acetone contents of 80, 60, 40, 35, 30, 25, 20, 10 wt. % in the precipitation solution. The last fraction F_8 is finally obtained by solvent evaporation. Earlier we found, that a minor amount of the starting lignin is not soluble in 80 wt. % acetone, which is separated (and defined as F_0) before the actual fractionation starts. Furthermore, we observed that during the first anti-solvent precipitation step (80 to 60 wt. % acetone) only a marginal amount is precipitated, which showed minor differences to the parent lignin concerning molecular weight and functionality [20]. Therefore, F_1 is not further taken into account for the characterization and discussion in this study. Further fractionation conditions, equilibration times, and phase separation can be found in detail in the earlier work [20].

2.3. Klason lignin, elemental analysis, ash and moisture content

The Klason lignin analysis was performed according to the National Renewable Energy Laboratory (NREL) standard analytical procedure [49]. A Flash 2000 CHNS&O Analyzer (ThermoFisher) was used for elemental analysis with a max. 5 mg sample to determine the C/H/N/S content. 2,5-Bis-(5-*tert*-butyl-benzooxazol-2-yl)thiophene (BBOT) served as a standard. Combustion and reduction tubes were operated at 900 °C with oxygen and helium flow at 140 ml min^{-1}. Each analysis was repeated three times. The oxygen content in the sample was determined by subtraction from 100 %. The ash content was determined by a laboratory chamber furnace (Carbolite CWF 13/23, Carbolite Gero) with a temperature ramp and combustion at 575 °C as described in the above-mentioned standard protocol [49]. The moisture content was

determined after freeze drying (VaCo 2, Zirbus Technology) of the lignin sample for 24 h until constant weight was reached.

2.4. SEC-MALS analysis

The MWD of the lignin samples was obtained by coupling three in series connected size exclusion chromatography (SEC) columns (Acetone-AQ-Phil-P 350 Å, 250 Å, and 150 Å, AppliChrom GmbH) with a multi angle light scattering detector (MALS) (Wyatt Technology Europe) as reported recently [20]. The wavelength of the laser light was 664 nm. Acetone, deionized water, and traces of formic acid were used as the eluent (79.2/19.8/1 vol. %). The flow rate was set at 1 ml min^{-1}. An injection volume of 100 µl and a sample concentration of 3 mg mL^{-1} were chosen. Additional information with respect to dissolving time, analysis, and interpretation of the chromatograms are described in previous work [20].

2.5. ^{31}P NMR spectroscopy analysis

Sample preparation of the lignin samples for quantitative ^{31}P NMR experiments followed the protocol of earlier methods. The analysis was performed on a Bruker 600 MHz spectrometer. Briefly, 30 mg of a lignin sample was dissolved in a mixture of pyridine/$CDCl_3$, and derivatization of the sample in 2-chloro-4,4,5,5-tetramethyl-1,3,2-dioxaphospholane concluded. Cholesterol served as the internal standard. The pulse program "zgig", 128 scans, the spectral width of 98 ppm, acquisition time of 1.38 sec, and a probe temperature of 298 K were selected. The OH content analyses were done using the quantitative approach as reported earlier [20,50].

2.6. Antioxidant activity

The DPPH (2,2-diphenyl-1-picrylhydrazyl) method according to Santos [48] can be used to demonstrate the antioxidant effect of lignin. The method has been slightly adapted for the analysis in this work. Different lignin sample concentrations were prepared using 90 vol. % dioxane. The samples are measured after dilution (1 to 40) with DPPH solution (23.65 g/l DPPH in methanol) in a cuvette by a UV/VIS spectrometer (Genesys 6, Thermo Fisher Scientific). The absorbance and inhibition of DPPH were recorded in triplicate at a wavelength of 517 nm. Trolox as a gold assay standard was tested on its radical scavenging activity. The inhibition strength was calculated as:

$$I = \frac{(Ab_0 - Ab_c)}{Ab_0} * 100 \quad (1)$$

where Ab_0 is the absorbance of the control (pure DPPH) and Ab_c is the absorbance of DPPH with the lignin sample or trolox.

2.7. Glass transition temperature analysis

Temperature-modulated differential scanning calorimetry (TM-DSC) was performed on a DSC 3 system (Mettler-Toledo) to investigate the thermal behavior, mainly the T_G of the lignin samples. Lignin samples (5–10 mg) were measured in solid state in pinned 40 µl aluminum crucibles. The temperature ramp was set from 25 to 250 °C with a heating rate of 1 °K min^{-1}. The nitrogen flow rate during the analysis was held at 30 ml min^{-1}. The evaluation of the TM-DSC data was conducted using the STARe software (Mettler Toledo) and T_G was determined by selecting the *"Midpoint ISO"* point for evaluation.

3. Results and discussion

3.1. Klason lignin and element analysis

The quality, respectively the purity of the parent lignin obtained from the relatively mild acetone OS process (Fabiola™) was analyzed by the Klason method, where lignin is divided into an acid soluble (AS) and an acid insoluble (AIS) lignin fraction. Table 1 summarizes the respective results for the parent lignin together with its ash and moisture content.

The purity of the processed lignin exceeds 95 wt. % and is comparable to other technical OS lignins [17,51]. However, the ash content found in this extracted beech wood lignin is negligibly small (<1 wt. %). Once including the moisture content, a minor residue of possible extractives (such as terpenes, flavonoids, oils, etc.) of less than 2 wt. % can be concluded. The parent lignin and the fractions F_0 and F_2 - F_8 of the 10 wt. % feed lignin fractionation row were analyzed on their elemental composition to further elaborate the quality with regard to nitrogen or sulfur traces. Fig. 1 displays the van Krevelen diagram for the aforementioned samples. The parent lignin and its fractions are located in a narrow range of O/C 0.37–0.41 and H/C 1.07–1.15. These values are typical for hardwood lignin and therefore represent polymeric lignin without any major indication of carbohydrates or proteins present [17]. Enlarging the lignin region in the van Krevelen diagram, it becomes visible that solely F_8 is slightly shifted to a lower degree of aromaticity (H/C 1.14; O/C 0.405). Furthermore, no traces of nitrogen or sulfur were detected, which supports the results from the Klason analysis revealing a high-quality pure lignin.

3.2. Impact of feed lignin concentration on precipitation behavior and solubility during stepwise anti-solvent precipitation fractionation

Fig. 2 displays the precipitated amount for the fractions F_0 to F_8 during the stepwise precipitation fractionation for all three fractionation rows. The amount of precipitation within a fractionation step at the same acetone concentration increases with higher feed lignin concentration for F_0 to F_2. The amount of the first (insoluble) fraction F_0 increases, respectively from 1.3 to 2.29 wt. %. Earlier we reported F_0 as non–soluble, potentially a fraction of impurities [20]. However, the van Krevelen plot in Fig. 1 clearly shows that F_0 lies in the same region as the other fractions and therefore likely represents a similar polymeric lignin sample as the others. The effect of co-solvent phenomena of certain lignin fractions on each other has not been studied in a broader subject in our work but current observations led to the hypothesis that F_0 may be a fraction of certain (high MW) lignin molecules that are not soluble in the mixture of 80 wt. % acetone/water, and the "purified parent lignin" (sum of the distribution from F_1 till F_8). These hypothetic conclusions of lignin co-solvent effects are supported by the findings by others [14,23]. The low yields of F_0 in Fig. 2 imply a good solubility of the parent lignin in 80 wt. % acetone. The reported solubility parameter for OS beech wood lignin of 25.5 $MPa^{1/2}$ [45] matches relatively well with the solubility parameter of the starting solvent system of 24.93 $MPa^{1/2}$ (pure acetone: 20.4 and water: 47.9 $MPa^{1/2}$ [53]). Similar high affinity for different OS lignins and this specific solvent mixture have been reported and support the results found here [10,25]. Throughout the precipitation fractionation procedure, the amount of the anti-solvent water increases stepwise, which leads to an increase of the solubility parameter of the lignin/solvent mixture towards water (47.9 $MPa^{1/2}$) [54]. The largest difference in precipitation quantity is found within the fractions, where the solubility decreases significantly. The precipitated amount in F_2 displays a 53 % higher yield for the 15 wt. % feed lignin in

Table 1
Analysis of Klason lignin, ash and moisture content of OS beech wood lignin.

	Organosolv beech wood lignin (wt. % on dry matter)
Total Klason Lignin	95.18
Acid Insoluble (AIS)	92.89 ± 0.04
Acid Soluble (AS)	2.29 ± 0.09
Ash content	0.035 ± 0.0002
Moisture content	3.13 ± 0.08

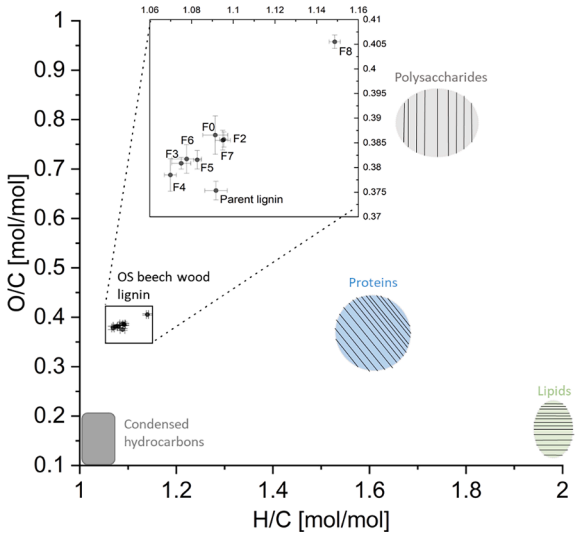

Fig. 1. Van Krevelen diagram displaying the elemental composition of the parent lignin and its fractions obtained for the 10 wt. % lignin feed fractionation row. Qualitative regions are displayed for cellulose (light grey), lipids (green), proteins (blue) and condensed hydrocarbons (dark grey).
adapted from [52]

comparison to the 5 wt. % feed lignin fractionation row. Starting from F_3, we observe a decrease in the yields for the fractions derived at higher feed lignin concentrations. Within the 15 wt. % feed lignin fractionation row, over 70 % of the lignin is precipitated within the first three fractionation steps (F_0 to F_3), and may explain its lower yields for the following fractions. Besides this, the decrease in yields from F_3 for all fractionation rows is likely explainable by the minor change in the acetone concentration (steps of 5 wt. % acetone) for the followings fractions, which were conducted after F_2.

For fractions 7 and 8, the yields increased again for all three fractionation rows in comparison to the previous fractions as the amount of anti-solvent was increased (steps of 10 wt. % acetone). Similar decreasing lignin precipitation yields with increasing water and different fractionation steps have been found earlier and support these results [10,25]. Depending on the fractionation row, 94–96 % of the starting lignin was recovered. The absolute masses are listed in Table S1. In [22], using a similar fractionation procedure, losses of ~20 % were registered even when the initial lignin mass was approx. 300 g.

3.3. Impact of stepwise anti-solvent precipitation fractionation on MW

The obtained fractions, namely the parent lignin separated from the non–soluble fraction F_0 (purified parent lignin; P.L.) and fractions F_1 to F_8 of all three fractionation rows were analyzed by SEC-MALS. The specific incremental refractive indices for each fraction (listed in Table S2) were determined beforehand to analyze the MWD and its average moments as accurate as possible. In Fig. 3 the weight average molecular weight (M_w) is displayed against the acetone concentration.

Note, that the M_w of F_1 obtained at 60 wt. % acetone is very similar to the purified parent lignin and hence not further discussed in this work as stated and reported earlier [20]. From F_2, respectively at 40 wt. % acetone, a clear monotonic trend towards lower M_w with increasing water content is noticeable for each fractionation row. The solubility of lignin(s) decreases as the acetone concentration reduces due to the gradual polarity shift of the solvent mixture during the stepwise fractionation precipitation process, whereby the solubility of each fraction changes differently due to different MWDs and phase compositions [14,23]. Generally, when the polarity increases, larger lignin molecules, which are less polar, tend to precipitate. Additionally, independently from the polarity, larger molecules follow a lower solubility than smaller molecules in the same solvent system. However, as stated earlier the MW is not the only factor that describes the solubility behavior of such polydisperse system. Similar MW trends by tuning the gradient of polarity in acetone–water mixtures have been previously documented [10,20,25,26].

Further, it becomes obvious that the M_w in each fraction is lower towards higher feed lignin concentrations. For the purified parent lignin it varies from 9360 g mol^{-1} (15 wt. % feed lignin) to 12800 g mol^{-1} (5 wt. % feed lignin). The difference within a fraction is most significantly visible for F_2. Hereby, the M_w values increase from 14450 (15 wt. % feed lignin) to 26500 g mol^{-1} (5 wt. % feed lignin). The differences in M_w within the fractions decrease slightly towards the latter fractions.

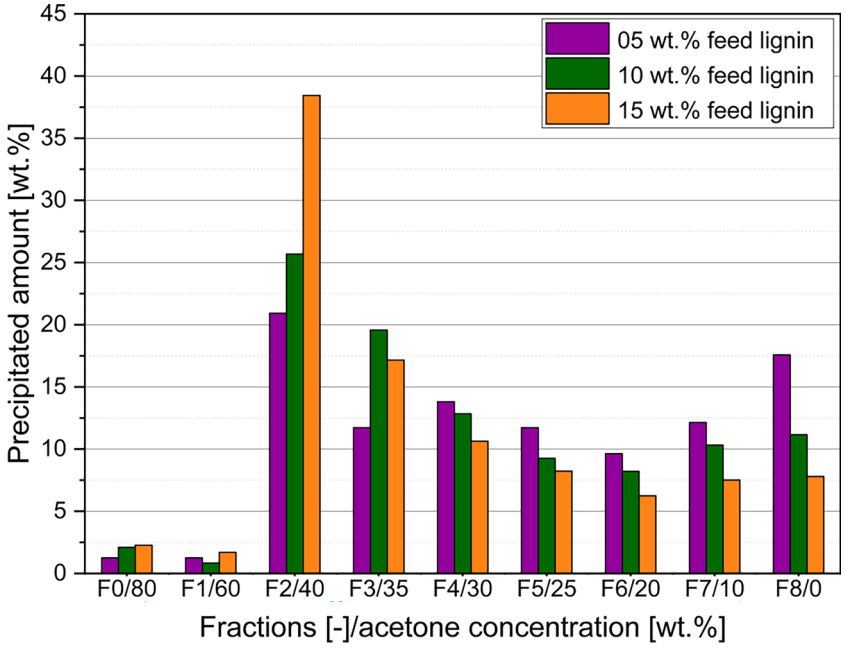

Fig. 2. Precipitated amount of each fraction for three different feed lignin fractionation rows. On the x-axis the fraction is given together with its specific acetone concentration (e.g. F0/80 corresponds to F_0 at 80 wt. % acetone).

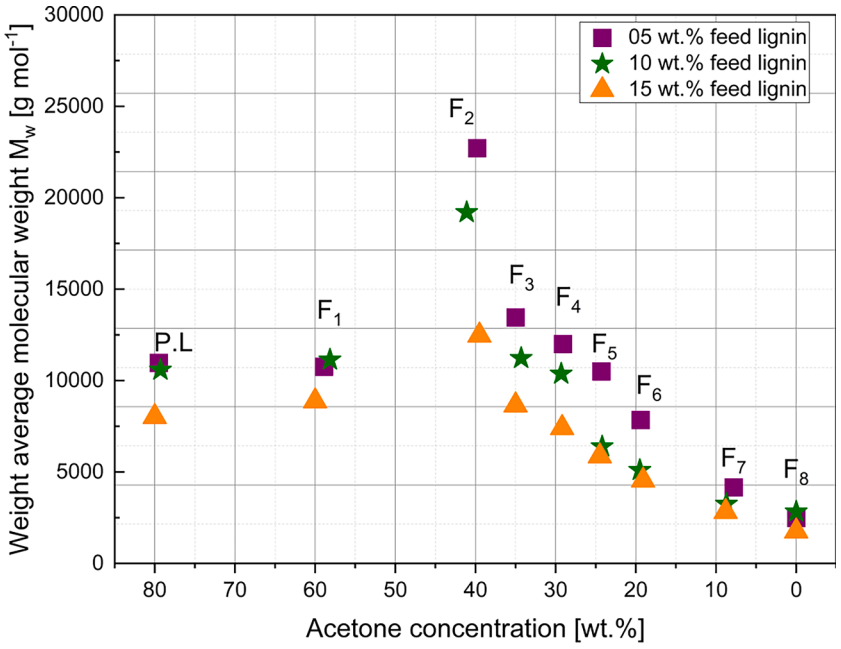

Fig. 3. M_W of the different obtained fractions for three fractionation rows plotted against the acetone concentration.

Nevertheless, the differences are still remarkable for fractions 3 to 6, presenting the largest difference of 44 % in F_5 between the 15 wt. % and 5 wt. % feed lignin fractionation row. The last fraction F_8 is in the M_w range between 2050 and 3300 g mol^{-1}. In Table 2 , the number average molecular weight (M_n), M_w, and dispersity (D) are summarized for all fractions.

The Fig. 4 illustrates the influence of the lignin concentration on the M_w of the obtained lignin fractions. Hereby, the M_w is plotted against the specific lignin concentration from which the fractions are separated.

The lignin concentrations were determined after phase separation occured and after each incremental addition of water. The black lines in Fig. 4 are isopleths of the acetone content as the acetone steps are equal in each fractionation row. The almost linear dependency between the lignin concentration and M_w is noticeable. Both, Fig. 3 and Fig. 4, reveal distinctly that the initial and consequently the following lignin concentration during the fractionation procedure have a significant impact on the solubility of the present lignin MWD and consequently on the final lignin MWs found in each fraction, respectively in the polymer-rich and polymer-lean phase.

It is well understood from classical polymer fractionation that the initial polymer concentration has an impact on the phase separation, leading to different compositions and thus MWs in each phase [41]. Hereby, a decrease in the average MW of the polymer-rich fraction was reported by initial higher polymer concentration in a system of solvent and two polymer-homologous species, in which one represents the smaller polymer molecules and the other larger polymer molecules. Additionally, lowering of the initial polymer concentration reduces the dispersity of the MWD in the polymer-rich phase. These conclusions based on two defined polymer species should be at least qualitatively valid for a polydisperse polymer in a solvent/anti-solvent mixture [41]. The listed dispersity values for each fraction in Tab. 2 also support this trend for the studied lignin/acetone/water system. With increasing lignin feed concentration, the dispersity in the fractions increases as well. The values rise for the purified parent lignin from 1.55 (5 wt. % feed lignin solution) to 1.78 (15 wt. % feed lignin solution). For F_2, an increase from 1.28 to 1.43 in the lignin feed concentration range studied is found. Therefore, these results prove that lignin behaves similarly to synthetic polymers during precipitation fractionation, whose fractionation behavior is well described in the literature [41]. The influence of the initial polymer concentration and a similiar MW trend have also been found for much higher (Kraft) lignin concentrations (14 and 25 wt. %) in ethanol/water and acetic/water systems. [14,23].

3.4. Impact of stepwise anti-solvent precipitation fractionation on glass transition temperature

With the variety in MW for each fraction, subsequently the impact on the T_G was investigated. Many factors influence the T_G of lignin, including its chemical structure (such as functional groups, linkage distributions, and linearity), purity, MW, and dispersity [55]. Among these factors, the chemical structure plays a crucial role in the softening capacity of lignin. For the processed OS beech wood lignin in this work,

Table 2
Absolute average molecular weights [kg/mol] and dispersity D [-] values obtained during fractionation for three different initial lignin feed concentrations (5, 10 and 15 wt. %).

-	M_n [5 wt. %]	M_n [10 wt. %]	M_n [15 wt. %]	M_w [5 wt. %]	M_w [10 wt. %]	M_w [15 wt. %]	D [5 wt. %]	D [10 wt. %]	D [15 wt. %]
P.L	8.3 ± 0.14	7.10 ± 0.28	5.25 ± 0.49	12.8 ± 0	12.35 ± 0.35	9.35 ± 0.35	1.55	1.73	1.78
F_2	20.70 ± 0.42	16.35 ± 1.62	10.20 ± 0	26.5 ± 0.21	22.30 ± 0.28	14.55 ± 0.21	1.28	1.37	1.43
F_3	14.45 ± 0.78	11.35 ± 0.21	8.5 ± 0.14	15.7 ± 0.71	13.1 ± 0.28	10.10 ± 0.14	1.09	1.15	1.19
F_4	13.15 ± 0.92	10.85 ± 0.49	6.8 ± 0.28	14 ± 0.99	12.1 ± 0.42	8.65 ± 0.21	1.07	1.11	1.27
F_5	10.85 ± 0.78	6.6 ± 0.14	5.1 ± 0.42	12.25 ± 1.06	7.40 ± 0.28	6.85 ± 0.21	1.13	1.12	1.35
F_6	8.3 ± 0.42	4.5 ± 0	3.9 ± 0.14	9.15 ± 0.49	5.95 ± 0.07	5.3 ± 0.14	1.10	1.32	1.37
F_7	3.70 ± 0.28	2.65 ± 0.07	2.15 ± 0.07	4.85 ± 0.07	3.8 ± 0.14	3.3 ± 0	1.31	1.42	1.53
F_8	2.35 ± 0.07	2.7 ± 0.28	1.40 ± 0.14	2.9 ± 0.0	3.3 ± 0.42	2.05 ± 0.07	1.24	1.20	1.45

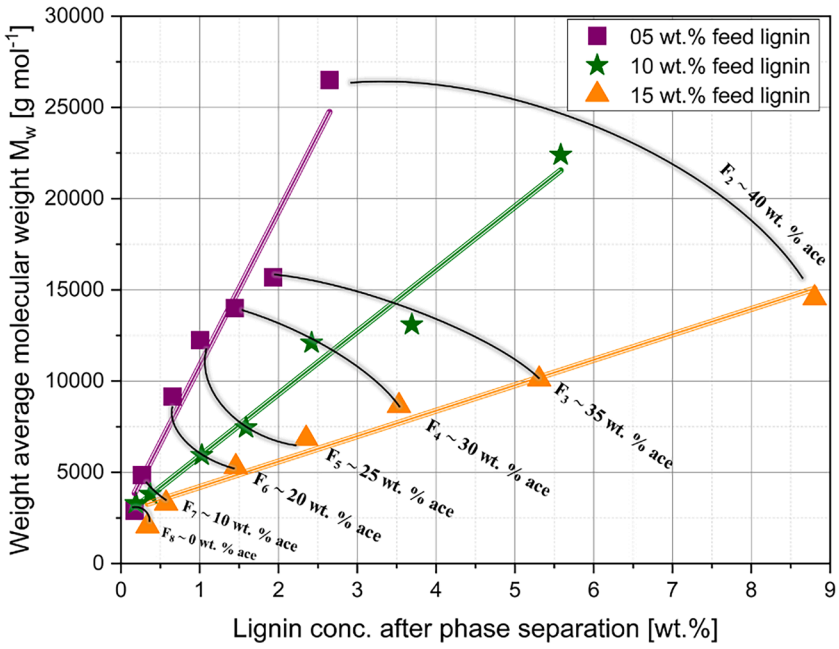

Fig. 4. M_w of the obtained fractions F_2 – F_8 plotted against the lignin concentration present after phase separation occurred for all three fractionation rows (black line represents qualitatively the isopleths of acetone).

glass transition temperatures were clearly verified for all fractions.

In Fig. 5a, the T_G values determined for the different lignin fractions are shown as a function of the number weight average molecular weight M_n. The glass transition temperatures decrease steadily from F_2 to F_8 for all three fractionation rows. The fractions lay in the T_G range between 68 and 201 °C. A summary of the T_G data is given in Table S3. Each glass transition temperature was determined in duplicate and deviations lower than ± 1.5 °C were observed. In general, the larger a (lignin) polymer molecule is, the more intramolecular bonds it consists of. Since these are more stable than intermolecular forces between molecules, more energy is required to transform the molecule from a glassy into a rubbery/softening state. Although, the purified parent lignin samples do not differ notably (Table S2), starting from F_2 significant differences between the three different fractionation rows can be found. Similar to the monotonic trend in the M_w plot (Fig. 3), the absolute differences in T_G for each fraction decrease towards the end of the fractionation (see Table S3), respectively revealing a T_G range for F_8 from 68 to 80 °C. The differences in F_2 are (absolutely) slightly higher from 181 to 201 °C.

In polymer chemistry, the glass transition temperature of amorphous polymers can be predicted using the Flory-Fox equation, which takes M_n into account:

$$T_G(M_n) \approx T_{G,\infty} - \frac{K}{M_n} \quad (2)$$

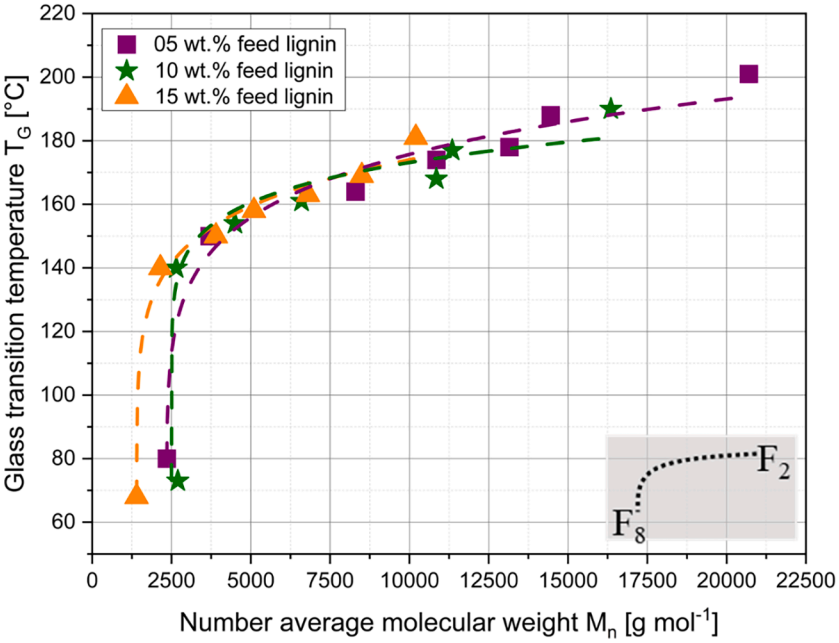

Fig. 5a. Glass transition temperature plotted against the number weight average molecular weight M_n for F_2 – F_8 for all three fractionation rows. Fractions are not individually indicated as this would overfill the figure. The overall trend is indicated on the bottom right in a grey box. Dashed line as guide for the eye only.

where $T_{G,\infty}$ is the limiting value of the T_G at very high MWs and K represents a constant considering the free volume for a given polymer (only for high MWs) [56]. According to equation (2), T_G increases with an increase in MW and eventually reaches a plateau at moderate to high molecular weights. However, the accuracy of this equation is limited when applied to the entire range of MWs, particularly for the lower range [56]. The equation describes many polymers, mostly linear polymers of low dispersity and uniform functional group distributions throughout the entire molar mass distributions of the sample. These conditions cannot be consistently found in lignins [27]. Nevertheless, the dashed lines for the lignin fractions in Fig. 5a follow a typical Flory-Fox course, although the M_n values are here rather small. Ogawa modified the Flory-Fox equation to obtain better accuracy for samples with broad MWD by including the M_w value [57]. Although plotting different representations (Fig. 5b, Fig. S1 and Fig. S2) no clear linear dependency throughout the whole range (one could put a linear trend for the first five data points in Fig. 5b) could be observed as for synthetic polymers, and no reliable values for K or $T_{G,\infty}$ could be identified within the lignin fractions. The outliers in Fig. 5b display the last fraction F_8 with the lowest MW, which may be too low to be considered in the modified Flory–Fox (Ogawa) equation.

The course in Fig. 5a may explain the polymeric behavior of lignin in general, however, its inherent complexity (variety in conformation, broad distribution, functionality) limits the usage of further predictions by these rather simple empirical models. A significant difference between F_7 and F_8 (the first two fractions) in Fig. 5a is visible. Although the M_w change between these fractions is comparable to the other ones, the glass transition temperatures of F_8 (68 to 80 °C) are with up to 52 % substantially lower than found of F_7 (140–150 °C). The glass transition temperature depends on further parameters such as the number of side chains in the polymer or the flexibility of the polymer molecules [58]. The free volume of a system can be among other parameters described by the number of polymer chain ends present in a sample. In a polymer sample with long chain lengths (high MW) and low dispersity, the total number of chain ends is lower, resulting in less free volume. Conversely, a polymer sample consisting of lower MW will have more chain ends. As a general rule, an increase in chain ends leads to a decrease in T_G. Further, the stiffer and branched a (bio)-polymer is, the higher its glass transition temperature [58]. Bing Li et al. have reported that the number of the major linkage, β-O-4, reduces by solvent fractionation in ethanol/water mixtures [59]. Gaspar et al. further found a decrease in the linkages of β-O-4, β- β, and β-5 with decreasing MW of lignin fractions obtained by sequential anti-solvent fractionation of hydrotropic Kraft lignin with the addition of water [60]. The NMR results found in this study (Tab. S4) support this trend. The number of free functional groups (higher free volume) is up to 45 % higher in the lower MW fractions than in the high ones (see also next section). These observations may explain the lower MW and the consequent glass transition temperature obtained in this fractionation procedure. It is noteworthy to mention, that such broad classification in T_G for untreated/non-modified hardwood OS lignin as processed here, including the shown MW–T_G correlation are notably and (to the best of authors knowledge) have not been reported before in such detail. The possibility to obtain target T_G ranges is prone to be more attractive for more specific polymer blends and formulations [61]. For example, concerning lignin-based carbon fibers, it has been reported that a higher T_G leads to better carbon fibers (strengths) [34].

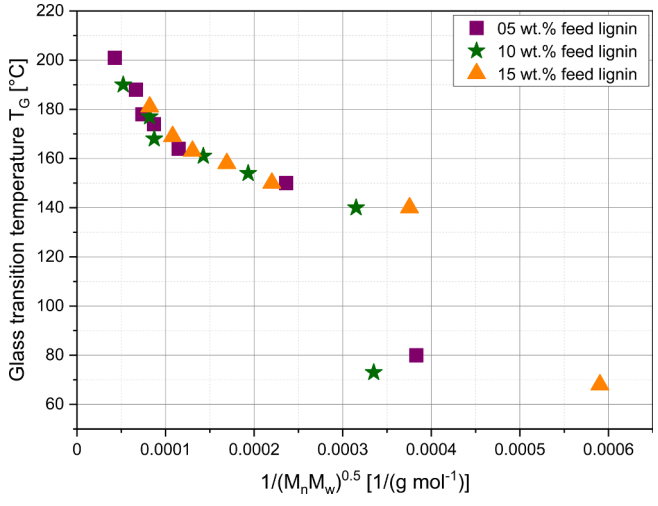

Fig. 5b. Glass transition temperature plotted against the inverse of the product of M_n and M_w (Flory-Fox (Ogawa)) for F_2 - F_8 of all three fractionation rows.

3.5. *Impact of stepwise anti-solvent precipitation fractionation on functionality*

The harvested fractions were further analyzed on their amount of carboxyl, aliphatic, and phenolic hydroxyl groups via ^{31}P NMR. By classification in different MWs, the functional dimension reveals a distribution and hence a scattering as well. In Fig. 6 the carboxyl (bottom greyed block), aliphatic (middle greyed blocked), and phenolic hydroxyl amounts (upper data points without a greyed block) in mmol per g_{lignin} are displayed for F_2 till F_8 for all three fractionations rows.

It is noticeable, that the phenolic OH content reveals the highest amount of free hydroxyl groups and exhibits a range from 2.05 to 4.26 mmol per g^{-1}_{lignin}. The aliphatic OH content ranges from 1.74 to 2.11 mmol g^{-1}_{lignin}, while the carboxyl OH amount shows the lowest amount below 0.5 mmol g^{-1}_{lignin} for all fractions in all fractionation rows. Whereas the differences within the fractions for the aliphatic and carboxyl regions are not that strong, tremendous differences within the fractions and lignin feed concentration are found in the phenolic hydroxyl region. The phenolic OH content increases from F_2 towards F_8 for all three feed lignin fractionation rows. The fractionation row with the lowest feed lignin concentration (5 wt. %) and the highest M_w exposes the lowest value in each fraction (2.05 – 3.66 mmol g^{-1}_{lignin}). Further, Fig. 6 reveals that the phenolic OH content is the highest for almost every fraction in the 10 wt. % feed lignin solution. Solely, F_8 of the 15 wt. % feed lignin fractionation row shows a higher value of 4.26 mmol g^{-1}_{lignin}. This is over 50 % more free phenolic OH groups than found in F_2 of the lowest (5 wt. %) feed lignin fractionation row. The observed trend in decreasing phenolic OH amounts with increasing M_w seems plausible as 50 to 60 % of the inter-unit linkages in hardwood lignin are found in the β-O-4 linkage [62]. A complete listing of all obtained NMR values is given in Tab. S4.

To increase the value of lignin, fractions with more accessible OH groups, especially aliphatic and phenolic OH groups can be attractive for higher-value applications. Lignin comes with natural antioxidant and antibacterial characteristics. A significant role during the scavenging effect is based on the methoxy and phenolic group structure. Hence, the scavenging effect of the purified parent lignin, and exemplary of F_5 and F_8 of the 10 wt. % feed lignin fractionation row were investigated and the values were compared with trolox, as a gold standard. The results are shown in Fig. 7 depicting the inhibition of DPPH for three different time points (10, 30, and 45 min). Trolox, a monodisperse and small molecule neutralizes quickly and exhibits an inhibition of 95 % already after 10 min. The inhibition increases for the lignin samples from the parent towards F_8, with an inhibition of 80 and 83 % after 10 and 45 mins, respectively. This trend underlines the results from the NMR analysis, representing higher reactivity due to functionality in samples of smaller MW fractions. In comparison to trolox, a kinetic dependency is observed for all lignin samples. This is again probably caused by the dispersity of lignin as not only do functional groups play a major role during the scavenging of DPPH but also most likely the steric hindrance.

Thus, the distributed lignin samples react further with DPPH and additional inhibition is registered with time. The flexibility and tuneability in functional groups can be very promising for certain

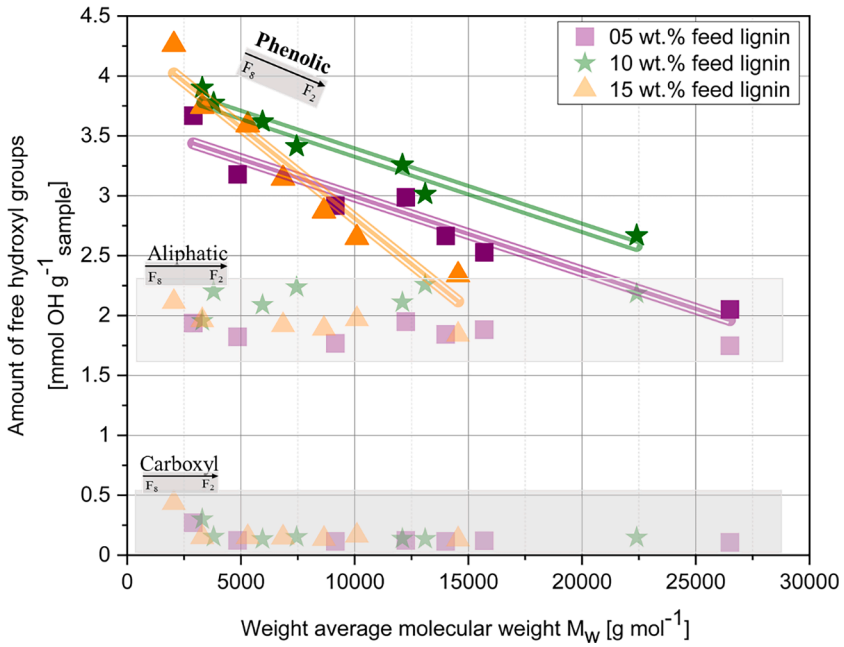

Fig. 6. Free carboxyl (bottom greyed box), aliphatic (middle greyed box) and phenolic (upper data points without greyed box) OH groups determined for F_2 – F_8 of all three fractionation rows. Arrows for each group indicate the general trend of the fractions with respect to their amounts of free hydroxyl groups.

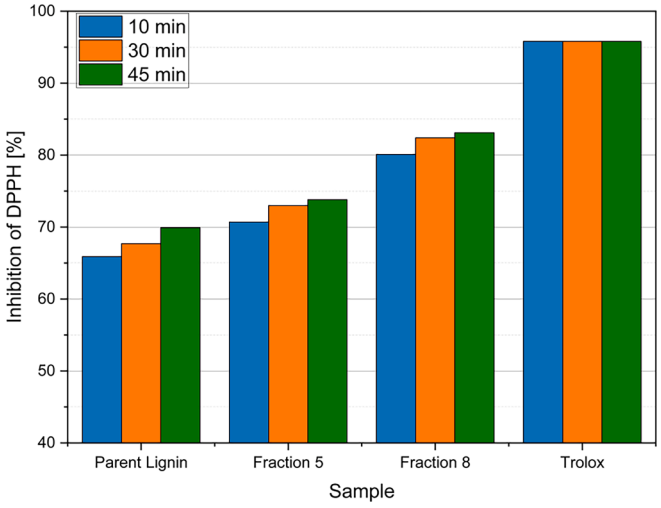

Fig. 7. Inhibition of DPPH by the purified parent lignin, F_5, F_8 and trolox of the 10 wt. % feed lignin fractionation row after 10, 30 and 45 minutes.

applications. The antibacterial and antioxidant properties of lignin are attractive for the food and health sector. Hereby, bio-based products with high phenolic content and consequently lower MW among other parameters (e.g. solubility) are desirable. Further, lignin is a natural UV blocker with huge potential for usage in sunscreens. Hereby, the current visual appearance of lignin limits the production of lignin-based sunscreens. However, it was shown that with efficient fractionation and following modification of the fractions both reduction of the dark color and an improved sun-blocking activity was achieved [63]. Lignin-based polyurethane foams have been under research for a while. Here, the interplay between aliphatic and phenolic OH groups is important [39,64]. The obtained NMR results demonstrate that different amounts of aliphatic/phenolic ratios can be produced, which is e.g. attractive for the substitution of synthetic polyols in the polyurethane (PU) foam production. Recently, Henry et al. reported the implementation of low MW lignin, which accounted for 80 % substitution of polyols in rigid PU foams [30]. The amounts of lignins needed for PU foam formulation are relatively high (e.g. 19 wt. % in [30]). The sequential precipitation demonstrated in this work shows low mass yields due to the large number of fractions. To increase absolute yields one could e.g. start with a higher lignin amount in the beginning of the fractionation procedure or by reducing the number of fractions during the fractionation. However, the latter leads probably to a higher dispersity of the fractions, which subsequently impact the MW, its distribution and the functionality.

4. Conclusion

Different lignin feed concentrations were prepared to investigate the effect of lignins dispersity during stepwise solvent/anti-solvent precipitation fractionation. The lignin concentration in each stage affected the solubility and phase separation of the obtained lignin fraction with its particular MWD during the fractionation process. Hence, this is addressed as another process parameter for tailoring lignin fractions with specific physicochemical characteristics. The lignin concentration, T_G, the amount of free OH groups and the scavenging activity correlated notably with the MW of the fractions. This work demonstrates the significance of the feed lignin concentration (wt. %) in the lignin/solvent/anti-solvent mixture (in addition to solvent selection) on the lignin fractionation process and enhances the understanding of lignins structure–property correlations.

CRediT authorship contribution statement

Arulselvan Ponnudurai: Conceptualization, Methodology, Software, Validation, Visualization, Writing – original draft, Writing – review & editing. **Peter Schulze:** Conceptualization, Investigation, Methodology, Supervision, Visualization, Writing – review & editing. **Andreas Seidel-Morgenstern:** Funding acquisition, Project administration, Resources, Writing – review & editing. **Heike Lorenz:** Project administration, Resources, Supervision, Writing – review & editing.

Declaration of competing interest

The authors declare that they have no known competing financial

interests or personal relationships that could have appeared to influence the work reported in this paper.

Data availability

Data will be made available on request.

Acknowledgements

The authors thank the European UNRAVEL project consortium, especially the Fraunhofer Institute for CBP in Leuna, Germany, and TNO from Petten, The Netherlands, for providing beech wood OS lignin samples. We further thank Markus Ikert and Anne Christin Reichelt from the Department of Process Systems Engineering for analyzing the ash content and performing the elemental analysis of the lignin samples. Also, we acknowledge Dr. Liane Hilfert from the Institute of Chemistry at the University of Magdeburg for running ^{31}P NMR experiments. We are thankful to Jacqueline Kaufmann and Stefanie Oberländer for their help in SEC and DSC measurements. This research is supported by the International Max Planck Research School for Advanced Methods in Process and Systems Engineering (IMPRS ProEng), Magdeburg, Germany.

Appendix A. Supplementary data

Supplementary data to this article can be found online at https://doi.org/10.1016/j.seppur.2024.126343.

References

[1] M.Y. Balakshin, E.A. Capanema, I. Sulaeva, P. Schlee, Z. Huang, M. Feng, M. Borghei, O.J. Rojas, A. Potthast, T. Rosenau, New opportunities in the valorization of technical lignins, ChemSusChem 14 (2021) 1016–1036.
[2] J. Xu, C. Li, L. Dai, C. Xu, Y. Zhong, F. Yu, C. Si, Biomass fractionation and lignin fractionation towards lignin valorization, ChemSusChem 13 (2020) 4284–4295.
[3] R. Rinaldi, R. Jastrzebski, M.T. Clough, J. Ralph, M. Kennema, P.C.A. Bruijnincx, B. M. Weckhuysen, Paving the way for lignin valorisation: recent advances in bioengineering, biorefining and catalysis, Angew. Chem. Int. Ed. 55 (2016) 8164–8215.
[4] R. Vanholme, B. Demedts, K. Morreel, J. Ralph, W. Boerjan, Lignin biosynthesis and structure, Plant Physiol 153 (2010) 895–905.
[5] J. Ralph, C. Lapierre, W. Boerjan, Lignin structure and its engineering, Curr. Opin. Biotechnol. 56 (2019) 240–249.
[6] M. Balakshin, E.A. Capanema, X. Zhu, I. Sulaeva, A. Potthast, T. Rosenau, O. J. Rojas, Spruce milled wood lignin: linear, branched or cross-linked? Green Chem. 22 (2020) 3985–4001.
[7] I.V. Pylypchuk, M. Karlsson, P.A. Lindén, M.E. Lindström, T. Elder, O. Sevastyanova, M. Lawoko, Molecular understanding of the morphology and properties of lignin nanoparticles: unravelling the potential for tailored applications, Green Chem. 25 (2023) 4415–4428.
[8] P.K. Mishra, A. Ekielski, The self-assembly of lignin and its application in nanoparticle synthesis: a short review, Nanomaterials (Basel, Switzerland) 9 (2019).
[9] M. Mohan, K. Huang, V.R. Pidatala, B.A. Simmons, S. Singh, K.L. Sale, J. M. Gladden, Prediction of solubility parameters of lignin and ionic liquids using multi-resolution simulation approaches, Green Chem. 24 (2022) 1165–1176.
[10] H. Sadeghifar, A. Ragauskas, Perspective on technical lignin fractionation, ACS Sustain. Chem. Eng. 8 (2020) 8086–8101.
[11] A.T. Smit, M. Verges, P. Schulze, A. van Zomeren, H. Lorenz, Laboratory- to pilot-scale fractionation of lignocellulosic biomass using an acetone organosolv process, ACS Sustain. Chem. Eng. 10 (2022) 10503–10513.
[12] T. Iversen, S. Wännström, Lignin-carbohydrate bonds in a residual lignin isolated from pine kraft pulp, Holzforschung 40 (1986) 19–22.
[13] W. Fang, M. Ståhl, O. Ershova, S. Heikkinen, H. Sixta, Purification and characterization of kraft lignin, Holzforschung 69 (2015).
[14] O. Agede, M.C. Thies, Purification and fractionation of lignin via alpha: liquid-liquid equilibrium for the lignin-acetic acid–water system, ChemSusChem n/a (2023) e202300989.
[15] P. Schulze, M. Leschinsky, A. Seidel-Morgenstern, H. Lorenz, Continuous separation of lignin from organosolv pulping liquors: combined lignin particle formation and solvent recovery, Ind. Eng. Chem. Res. 58 (2019) 3797–3810.
[16] P.P. Thoresen, L. Matsakas, U. Rova, P. Christakopoulos, Recent advances in organosolv fractionation: towards biomass fractionation technology of the future, Bioresour. Technol. 306 (2020) 123189.
[17] C. Rasche, R. Janzon, B. Saake, M. Leschinsky, Effect of process parameters in pilot scale operation on properties of organosolv lignin, BioResources 14 (2019) 4543–4559.
[18] P. Schulze, A. Seidel-Morgenstern, H. Lorenz, M. Leschinsky, G. Unkelbach, Advanced process for precipitation of lignin from ethanol organosolv spent liquors, Bioresour. Technol. 199 (2016) 128–134.
[19] M. Leschinsky, G. Unkelbach, P. Schulze, H. Lorenz, A. Seidel-Morgenstern, Method for precipitating lignin from organosolv pulping liquors, in: E.P. Office (Ed.), Germany, 2017.
[20] A. Ponnudurai, P. Schulze, A. Seidel-Morgenstern, H. Lorenz, Fractionation and absolute molecular weight determination of organosolv lignin and its fractions: analysis by a novel acetone-based SEC—MALS method, ACS Sustain. Chem. Eng. 11 (2023) 766–776.
[21] L.A. Riddell, F.J.P.A. Enthoven, J.-P.-B. Lindner, F. Meirer, P.C.A. Bruijnincx, Expanding lignin thermal property space by fractionation and covalent modification, Green Chem. 25 (2023) 6051–6056.
[22] G. Tindall, B. Lynn, C. Fitzgerald, L. Valladares, Z. Pittman, V. Bécsy-Jakab, D. Hodge, M. Thies, Ultraclean hybrid poplar lignins via liquid–liquid fractionation using ethanol–water solutions, MRS Commun. 11 (2021) 692–698.
[23] G.W. Tindall, J. Chong, E. Miyasato, M.C. Thies, Fractionating and purifying softwood kraft lignin with aqueous renewable solvents: liquid-liquid equilibrium for the lignin–ethanol–water system, ChemSusChem 13 (2020) 4587–4594.
[24] A.S. Jääskeläinen, T. Liitiä, A. Mikkelson, T. Tamminen, Aqueous organic solvent fractionation as means to improve lignin homogeneity and purity, Ind. Crop. Prod. 103 (2017) 51–58.
[25] H. Sadeghifar, T. Wells, R.K. Le, F. Sadeghifar, J.S. Yuan, A.J. Ragauskas, Fractionation of organosolv lignin using acetone: water and properties of the obtained fractions, ACS Sustain. Chem. Eng. 5 (2017) 580–587.
[26] J. Domínguez-Robles, T. Tamminen, T. Liitiä, M.S. Peresin, A. Rodríguez, A.-S. Jääskeläinen, Aqueous acetone fractionation of kraft, organosolv and soda lignins, Int. J. Biol. Macromol. 106 (2018) 979–987.
[27] O. Musl, S. Galler, G. Wurzer, M. Bacher, I. Sulaeva, I. Sumerskii, A.K. Mahler, T. Rosenau, A. Potthast, High-resolution profiling of the functional heterogeneity of technical lignins, Biomacromolecules 23 (2022) 1413–1422.
[28] H. Haridevan, D.A.C. Evans, A.J. Ragauskas, D.J. Martin, P.K. Annamalai, Valorisation of technical lignin in rigid polyurethane foam: a critical evaluation on trends, guidelines and future perspectives, Green Chem. 23 (2021) 8725–8753.
[29] M.N. Collins, M. Nechifor, F. Tanasa, M. Zanoaga, A. McLoughlin, M.A. Strozyk, M. Culebras, C.A. Teaca, Valorization of lignin in polymer and composite systems for advanced engineering applications - a review, Int. J. Biol. Macromol. 131 (2019) 828–849.
[30] C. Henry, G. Tindall, M.C. Thies, M. Nejad, Fractionated and purified hybrid poplar lignins as a polyol replacement in rigid polyurethane/polyisocyanurate foams, J. Appl. Polym. Sci. 140 (2023) e54648.
[31] J. Jin, J. Ding, A. Klett, M.C. Thies, A.A. Ogale, Carbon fibers derived from fractionated-solvated lignin precursors for enhanced mechanical performance, ACS Sustain. Chem. Eng. 6 (2018) 14135–14142.
[32] S. Wang, J. Bai, M.T. Innocent, Q. Wang, H. Xiang, J. Tang, M. Zhu, Lignin-based carbon fibers: Formation, modification and potential applications, Green Energy Environ. 7 (2022) 578–605.
[33] Q. Li, W.K. Serem, W. Dai, Y. Yue, M.T. Naik, S. Xie, P. Karki, L. Liu, H.-J. Sue, H. Liang, F. Zhou, J.S. Yuan, Molecular weight and uniformity define the mechanical performance of lignin-based carbon fiber, J. Mater. Chem. A 5 (2017) 12740–12746.
[34] S.V. Kanhere, G.W. Tindall, A.A. Ogale, M.C. Thies, Carbon fibers derived from liquefied and fractionated poplar lignins: the effect of molecular weight, iScience 25 (2022) 105449.
[35] R. Liu, A. Smeds, L. Wang, A. Pranovich, J. Hemming, S. Willför, H. Zhang, C. Xu, Fractionation of lignin with decreased heterogeneity: based on a detailed characteristics study of sequentially extracted softwood kraft lignin, ACS Sustain. Chem. Eng. 9 (2021) 13862–13873.
[36] C.G. Boeriu, F.I. Fitigau, R.J.A. Gosselink, A.E. Frissen, J. Stoutjesdijk, F. Peter, Fractionation of five technical lignins by selective extraction in green solvents and characterisation of isolated fractions, Ind. Crop. Prod. 62 (2014) 481–490.
[37] V. Rohde, S. Boringer, B. Tubke, C. Adam, N. Dahmen, D. Schmiedl, Fractionation of three different lignins by thermal separation techniques-A comparative study, Glob. Change Biol. Bioenergy. 11 (2019) 206–217.
[38] X. Jiang, D. Savithri, X.Y. Du, S. Pawar, H. Jameel, H.M. Chang, X.F. Zhou, Fractionation and characterization of kraft lignin by sequential precipitation with various organic solvents, ACS Sustain. Chem. Eng. 5 (2017) 835–842.
[39] A. Duval, G. Layrac, A. van Zomeren, A.T. Smit, E. Pollet, L. Avérous, Isolation of low dispersity fractions of acetone organosolv lignins to understand their reactivity: towards aromatic building blocks for polymers synthesis, ChemSusChem 14 (2021) 387–397.
[40] J. Yan, E.C.D. Tan, R. Katahira, T.R. Pray, N. Sun, Fractionation of lignin streams using tangential flow filtration, Ind. Eng. Chem. Res. 61 (2022) 4407–4417.
[41] F. Francuskiewicz, Polymer Fractionation, Springer Science & Business Media, 1994.
[42] R.A. Miranda-Quintana, L. Chen, J. Smiatek, Insights into hildebrand solubility parameters – contributions from cohesive energies or electrophilicity densities? ChemPhysChem n/a (2023) e202300566.
[43] C. Hansen, Hansen Solubility Parameters: A User's Handbook, second ed., 2012.
[44] A. Dastpak, T.V. Lourenço, M. Balakshin, S. Farhan Hashmi, M. Lundström, B. P. Wilson, Solubility study of lignin in industrial organic solvents and investigation of electrochemical properties of spray-coated solutions, Ind. Crop. Prod. 148 (2020) 112310.
[45] H.Q. Lê, A. Zaitseva, J.-P. Pokki, M. Ståhl, V. Alopaeus, H. Sixta, Solubility of organosolv lignin in γ-valerolactone/water binary mixtures, ChemSusChem 9 (2016) 2939–2947.

[46] J. Sameni, S. Krigstin, M. Sain, Solubility of lignin and acetylated lignin in organic solvents, BioResources 12 (2017) 1548–1565.
[47] K. Wang, F. Xu, R. Sun, Molecular characteristics of Kraft-AQ pulping lignin fractionated by sequential organic solvent extraction, Int. J. Mol. Sci. 11 (2010) 2988–3001.
[48] P.S.B.D. Santos, X. Erdocia, D.A. Gatto, J. Labidi, Characterisation of Kraft lignin separated by gradient acid precipitation, Ind. Crop. Prod. 55 (2014) 149–154.
[49] A. Sluiter, B. Hames, R. Ruiz, C. Scarlata, J. Sluiter, D. Templeton, D. Crocker, Determination of structural carbohydrates and lignin in biomass, in: Laboratory Analytical Procedure (LAP), National Renewable Energy Laboratory, 2008.
[50] X. Meng, C. Crestini, H. Ben, N. Hao, Y. Pu, A.J. Ragauskas, D.S. Argyropoulos, Determination of hydroxyl groups in biorefinery resources via quantitative 31P NMR spectroscopy, Nat. Protoc. 14 (2019) 2627–2647.
[51] P. Jõul, T.T. Ho, U. Kallavus, A. Konist, K. Leiman, O.S. Salm, M. Kulp, M. Koel, T. Lukk, Characterization of organosolv lignins and their application in the preparation of aerogels, Materials (Basel, Switzerland) 15 (2022).
[52] A. Rivas-Ubach, Y. Liu, T.S. Bianchi, N. Tolić, C. Jansson, L. Paša-Tolić, Moving beyond the van Krevelen diagram: a new stoichiometric approach for compound classification in organisms, Anal. Chem. 90 (2018) 6152–6160.
[53] C. Schuerch, The solvent properties of liquids and their relation to the solubility, swelling, isolation and fractionation of lignin, J. Am. Chem. Soc. 74 (1952) 5061–5067.
[54] X. Li, J. Shen, B. Wang, X. Feng, Z. Mao, X. Sui, Acetone/water cosolvent approach to lignin nanoparticles with controllable size and their applications for pickering emulsions, ACS Sustain. Chem. Eng. 9 (2021) 5470–5480.
[55] R. Ebrahimi Majdar, A. Ghasemian, H. Resalati, A. Saraeian, C. Crestini, H. Lange, Case study in kraft lignin fractionation: "structurally purified" lignin fractions—the role of solvent h-bonding affinity, ACS Sustain. Chem. Eng. 8 (2020) 16803–16813.
[56] T.G. Fox, P.J. Flory, The glass temperature and related properties of polystyrene. Influence of molecular weight, J. Polym. Sci. 14 (1954) 315–319.
[57] T. Ogawa, Effects of molecular weight on mechanical properties of polypropylene, J. Appl. Polym. Sci. 44 (1992) 1869–1871.
[58] R. Xie, A.R. Weisen, Y. Lee, M.A. Aplan, A.M. Fenton, A.E. Masucci, F. Kempe, M. Sommer, C.W. Pester, R.H. Colby, E.D. Gomez, Glass transition temperature from the chemical structure of conjugated polymers, Nat. Commun. 11 (2020) 893.
[59] B. Li, M. Zhou, W. Huo, D. Cai, P. Qin, H. Cao, T. Tan, Fractionation and oxypropylation of corn-stover lignin for the production of biobased rigid polyurethane foam, Ind. Crop. Prod. 143 (2020) 111887.
[60] R. Gaspar, M. Muguet, P. Fardim, Advanced fractionation of kraft lignin by aqueous hydrotropic solutions, Molecules (Basel, Switzerland) 28 (2023).
[61] A. Beaucamp, Y. Wang, M. Culebras, M.N. Collins, Carbon fibres from renewable resources: the role of the lignin molecular structure in its blendability with biobased poly(ethylene terephthalate), Green Chem. 21 (2019) 5063–5072.
[62] X. Liu, F. Bouxin, J. Fan, V. Budarin, C. Hu, J. Clark, Recent advances in the catalytic depolymerization of lignin towards phenolic chemicals: a review, ChemSusChem 13 (2020).
[63] M.H. Tran, D.-P. Phan, E.Y. Lee, Review on lignin modifications toward natural UV protection ingredient for lignin-based sunscreens, Green Chem. 23 (2021) 4633–4646.
[64] A. Duval, D. Vidal, A. Sarbu, W. René, L. Avérous, Scalable single-step synthesis of lignin-based liquid polyols with ethylene carbonate for polyurethane foams, Mater. Today Chem. 24 (2022) 100793.